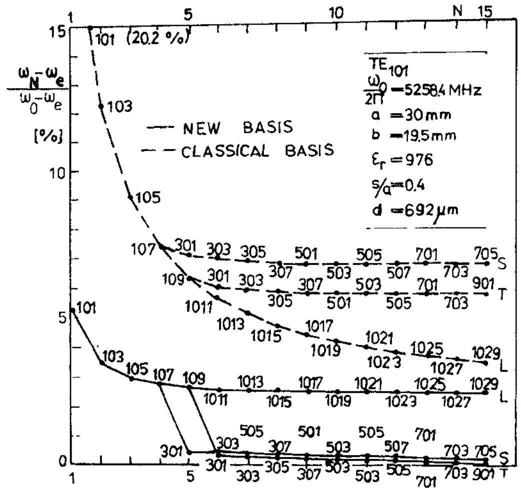

Fig. 2. Errors of frequency shift determination in quasi-TE_{101} cavity containing a sample width $s/a = 0.4$ for various sets of basis functions. The results are refered to the "exact" value of angular frequency shift. Numbers on the curves denote subscripts $i0k$ of TE_{i0k} basis functions (classical basis) and quasi-TE_{i0k} basis function (new basis).

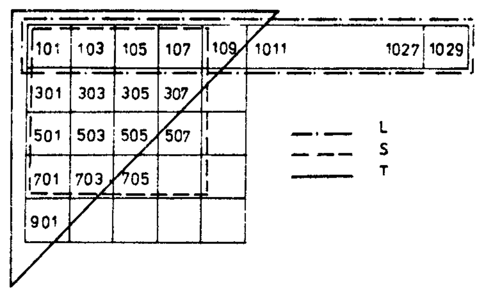

Fig. 3. Various sets of basis functions consisting of TE_{i0k} and quasi-TE_{i0k} modes.

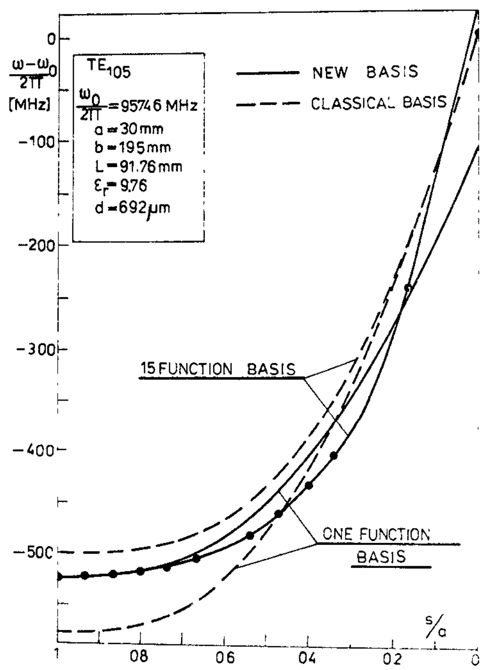

Fig. 4. Frequency shift of quasi-TE_{105} cavity calculated using various bases. a) The best new 15-function basis. b) The best classical 15-function basis. c) A new single-function basis. d) The classical single-function basis. The point denotes the experimental results.

tions of sets for classical and new bases denoted by letters L, T, S were used (Fig. 3). For each of the three configurations the number of basis functions was subsequently reduced to one in a sequence marked in Fig. 2. The three and four figure numbers on Fig. 2 and Fig. 3 denote subscripts $i0k$ of TE_{i0k} basis functions (classical basis—empty cavity modes) and quasi-TE_{i0k} basis functions (new basis).

It follows from Fig. 2 that the use of a new basis yields best results in the case of T configuration, whereas the classical basis yields the best results in the case of L configuration. The classical 15-function basis L provides the same calculations accuracy as the new basis composed of only two functions.

Fig. 4 presents the values of the frequency shift of a quasi TE_{105} cavity with samples of various width s, calculated for the best two 15-function bases among those compared in Fig. 2 (new and classical ones) and two single function bases. The experimental data are marked by points. The results of calculations and experiments confirm the results presented in Fig. 2.

IV. Conclusions

The performed calculations and measurements lead to the conclusion that the modification of the basis in the Galerkin method, presented in this paper, yields much more accurate results of calculations than the use of the classical basis (with some restrictions imposed on sample dimensions, mentioned in the paper). The presented method may find applications in the analysis of two-dimensional boundary problems for cavities with regular inhomogeneous filling. Such problems are typically encountered in the measurements of the permittivity of dielectrics.

References

[1] R F. Harrington, *Field Computation by Moment Methods* New York: MacMillan, 1968.

[2] V. V Nikolskij, "Variational methods for electrodynamic problems," *Science*, Moscow, 1967.

[3] R. Courant and D. Hilbert, *Methods of Mathematical Physics*. New York: Interscience, 1953.

[4] K. Mehmet and M. K. McPhun, "Measurement of the properties of rectangular plates using a rectangular cavity," in *Proc. Conf.: High Frequency Dielectric Measurement*. London: IPC Science and Technology Press, 1972.

[5] M. Sucher and J. Fox, *Handbook of Microwave Measurement*. New York: Polytechnic Press of PIB, 1963, Ch. 9.

The Conservation of Complex Power Technique and *E*-Plane Step-Diaphragm Junction Discontinuities

E. M. SICH, MEMBER, IEEE, AND R. H. MACPHIE, SENIOR MEMBER, IEEE

***Abstract*—The singular integral equation solution due to L. Lewin and his colleagues for the *E*-plane step-diaphragm junction discontinuity are extended by the conservation of complex power technique (CCPT). The singular integral equation method provides formulas for the junction susceptance (both with and without a diaphragm) which are valid only in the**

Manuscript received April 22, 1981; revised August 13, 1981. This work was supported by the Natural Sciences and Engineering Research Council (NSERC), Ottawa, Canada, under Grant A2176.

E. M. Sich is with Bell Northern Research, Terminals Development Division, P.O. Box 3511, Station C, Ottawa, Canada K1Y 4H7.

R H. MacPhie is with the Department of Electrical Engineering, University of Waterloo, Waterloo, Ontario, Canada N2L 3G1.

quasi-static limit. In contrast, the CCPT provides convergent numerical solutions for larger guides. It is also applied to a step with a diaphragm of nonvanishing thickness.

I. Introduction

In a recent paper [1] Ruehle and Lewin have presented an approximate solution, by the singular integral equation technique, to the waveguide problem of an E-plane step-diaphragm discontinuity combined with a change of media; the geometry is illustrated in Fig. 1. This is a generalization of earlier work on the E-plane step and simultaneous change of media [2]. Both papers employ the quasi-static approximation ([3], p. 265) and apply only to the case of the 2:1 step discontinuity.

Using TE and/or TM modal expansions for the fields on either side of a transverse plane junction of two waveguides, Safavi Naini and MacPhie [4] have shown recently that mode matching the transverse E-field at the junction and applying the principle of conservation of complex power yields a formally exact, numerically convergent solution to this type of scattering problem. Indeed the formulation leads to an expression for the complete scattering matrix $\boldsymbol{S}$, including scattering of higher order modes; since these modes form a complete set of basis functions for the waveguide fields the solution is exact.

However in practice the numerical computations dictate that $\boldsymbol{S}$ (obtained by a matrix inversion) be finite in size. Nevertheless a convergence analysis has shown [4] that if about ten modes are considered for the field expansion in the smaller waveguide the resulting solutions for the dominant mode reflection and transmission coefficients are accurate to about 2 or 3 significant figures in most cases.

In this paper we use the conservation of complex power technique (CCPT) to treat the same problems as those of Lewin and his colleagues and show that the singular integral equation–quasi-static method is valid (not surprisingly) only for junctions whose dimensions in terms of free space wavelengths are very small. Moreover we generalize the problems to include the cases of steps other than 2:1 and of diaphragms of nonvanishing thickness.

II. Formulation of the Problem

Consider the configuration shown in Fig. 2—a series connection of three parallel plate waveguides of widths b_1, b_2, and b_3 and with corresponding dielectric fillings with permittivities ϵ_1, ϵ_2, and ϵ_3. If the second guide is narrower than the first and third and is of length D, then it behaves as a thick capacitive diaphragm; as $D \to 0$ the geometry of Fig. 1 is obtained.

There are two transverse junction planes—A and B, as indicated in Fig. 2. Using the E-field mode matching and conservation of complex power technique [4] one can deduce the scattering matrices for each junction. Recalling that junction A separates guides 1 and 2, whereas junction B separates guides 2 and 3, it follows that the two scattering matrices can be written as

$$S_A = \begin{bmatrix} S_{11} & S_{12} \\ S_{21} & S_{22}^A \end{bmatrix} \qquad S_B = \begin{bmatrix} S_{22}^B & S_{23} \\ S_{32} & S_{33} \end{bmatrix} \tag{1}$$

where S_{ij}, for $i=1,2,3, j=1,2,3$ is the submatrix whose (r,k)th element is the scattered E-field amplitude for the rth mode in guide i due to a unit amplitude kth mode in guide j. Details of the derivation of the scattering matrices can be found in [4] for the case of TM modes, which are out present concern.

The effect of the central waveguide of length D can be accounted for by the diagonal transmission matrix $\boldsymbol{L}$ whose

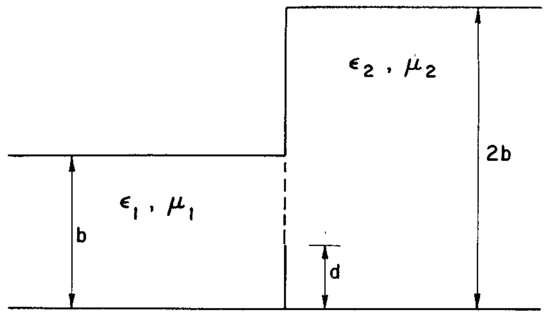

Fig. 1. Waveguide step with aperture diaphragm.

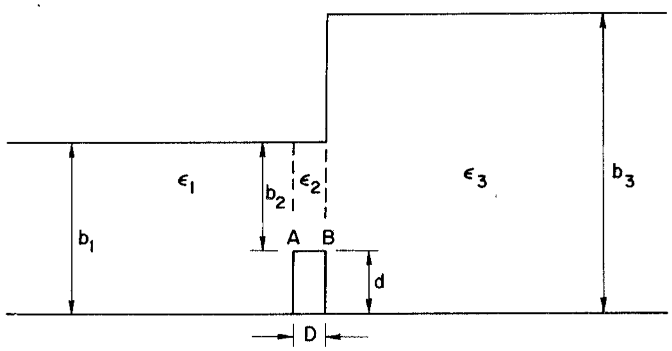

Fig. 2. Cascaded connection of three parallel plate waveguides.

elements are given by

$$l_{rq} = \exp\left\{ -j\sqrt{k_2^2 - (r\pi/b_2)^2}\, D \right\} \delta_{rq} \tag{2}$$

where

$$k_2 = \omega\sqrt{\epsilon_2 \mu_0}$$

ω being the radian frequency and μ_0 the permeability.

Using the generalized scattering-matrix technique ([5], pp. 207–217), it is straightforward to deduce the overall scattering matrix S^c of the cascaded junction

$$S^c = \begin{bmatrix} S_{11}^c & S_{13}^c \\ S_{31}^c & S_{33}^c \end{bmatrix} \tag{3}$$

where

$$S_{11}^c = S_{11} + S_{12} L S_{22}^A G_1 L S_{21} \tag{4}$$

$$S_{31}^c = S_{32} G_1 L S_{21} \tag{5}$$

$$S_{13}^c = S_{12} G_2 L S_{23} \tag{6}$$

and

$$S_{33}^c = S_{33} + S_{32} L S_{22}^B G_2 L S_{23}. \tag{7}$$

In (4)–(7) the G-matrices are as follows:

$$G_1 = \left(I - L S_{22}^A L S_{22}^B\right)^{-1} \tag{8}$$

and

$$G_2 = \left(I - L S_{22}^B L S_{22}^A\right)^{-1} \tag{9}$$

where I is the identity matrix. In the numerical computations, the results of which are given in the next section, the matrices are truncated to embrace 8 modes in guide 1 and 16 in guide 3.

III. Comparison with the Quasi-Static Solutions

The parameter treated by Lewin and his colleagues is the junction susceptance B, as "seen" by an incident TEM mode in guide 1. For the simpler geometry [2], where there is *no di-*

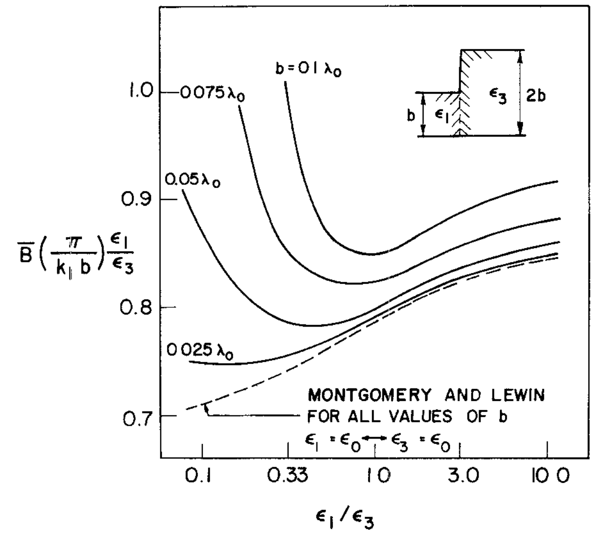

Fig. 3. Junction susceptance as a function of ϵ_1/ϵ_3 with b as a parameter.

aphragm and $b_3=2b_1$, they obtain the normalized formula

$$\bar{B}=\frac{B}{Y_1^0}\bigg|_{\text{no diaphragm}}=\frac{k_1b_1}{\pi}\alpha^2\frac{\epsilon_3}{\epsilon_1}\left[\frac{\pi}{2\alpha}-2\log 2-\psi(1-\beta)-\gamma\right] \tag{10}$$

where $\psi(x)$ is Euler's psi-function and γ is Euler's constant; $\alpha=\sqrt{1+2\epsilon_1/\epsilon_3}$ and $\pi\beta=\tan^{-1}(\alpha)$ with $0<\pi\beta<\pi$. Alternatively, the term in the square bracket in (10) can be written as $[\pi/2\alpha+\psi(1/2)-\psi(1-\beta)]$. For the more involved geometry with a diaphragm of zero thickness, height d, and again with $b_3=2b_1$ the formula is

$$\bar{B}=\frac{B}{Y_1^0}\bigg|_{\text{diaphragm}}=\frac{k_1b_1}{\pi}\alpha^2\frac{\epsilon_3}{\epsilon_1}\left[\frac{\pi}{2\alpha}-2\log 2-\psi(1-\beta)-\gamma-\log c\right] \tag{11}$$

where $c=\cos(\pi d/2b_1)$.

The CCPT provides the scattering matrix S^c and in particular $S^c_{11,00}$ which is the dominant TEM mode reflection coefficient in the first guide. It then can be shown that the junction susceptance B normalized with respect to the TEM admittance Y_1^0 is

$$j\bar{B}=j\frac{B}{Y_1^0}=\frac{1-S^c_{11,00}}{1+S^c_{11,00}}-\frac{Y_3^0}{Y_1^0}\left(\frac{b_1}{b_3}\right). \tag{12}$$

This equation is valid for the comparison case when the thickness D of the diaphragm is very much less than the free space wavelength and, of course, for the case when the diaphragm vanishes entirely.

Fig. 3 illustrates the latter case (no diaphragm) and only for $b_1=b<0.025\lambda_0$ is the quasi-static approximation quite accurate. Moreover, even for $b=0.10\lambda_0$ the quasi-static curve is in error by about 8 percent for $\epsilon_1>\epsilon_3$ and by very much more for $\epsilon_1<\epsilon_3$ when the junction's susceptance increases dramatically. A possible explanation is that as ϵ_3 increases the attenuation constants of the next higher order cutoff modes $(\text{TM}_1,\text{TM}_2,\cdots)$ decrease. This increases the volume of the larger guide where there is significant stored electric energy; this increasing volume is accompanied by an increase in the electric energy density $(W_e=(1/2)\epsilon_3|\vec{E}|^2)$ since ϵ_3 is also increasing. These two effects perhaps explain the large increase in the junction susceptance that is observed in Fig. 3 as ϵ_1/ϵ_3 falls below unity, an increase that is not predicted by the quasi-static formula. It is interesting to note that $\bar{B}$ in Fig. 3 is *quadratic* in b/λ_0 and agrees with formula (2c) on p. 308 of [6].

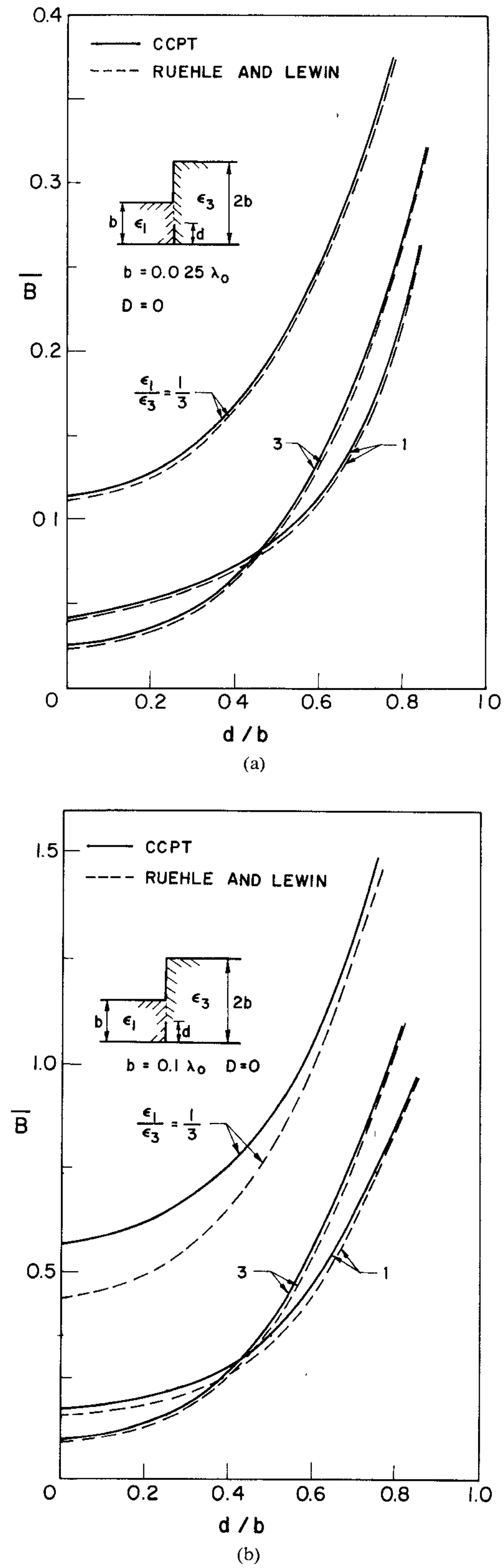

Fig. 4. Normalized junction susceptance as a function of d/b for (a) $b=0.025\lambda_0$, (b) $b=0.10\lambda_0$, with ϵ_1/ϵ_3 as a parameter and $D=0$.

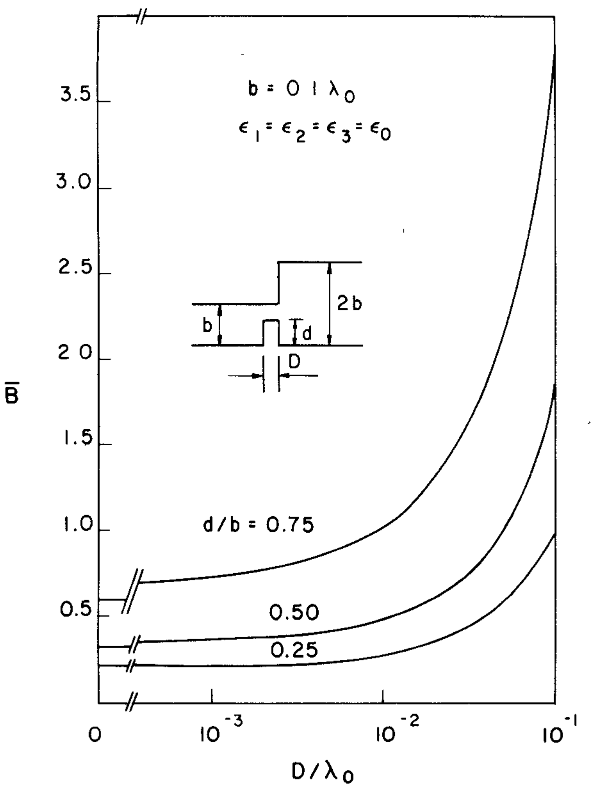

Fig. 5. Normalized junction susceptance as a function of D/λ_0 for $b = 0\ 10\lambda_0$ with d/b as a parameter and $\epsilon_1 = \epsilon_2 = \epsilon_3 = \epsilon_0$.

Turning now to the case of the diaphragm plus the E-plane step discontinuity we consider the special conditions of a 2:1 step and infinitesimally thin diaphragm and compare the quasi-static results [1] with those based on the conservation of complex power principle [4]. Fig. 4(a) shows that for *very small* spacings ($b_1 = b = 0.025\lambda_0$) the two methods give approximately the same solution for a wide range of dielectric constants and diaphragm heights. Fig. 4(b) considers a *small* spacing ($b_1 = b = 0.10\lambda_0$) and although the results are quite close when $\epsilon_1 = \epsilon_3$ and $\epsilon_1 = 3\epsilon_3$ there is a noticeable error in the quasi-static solution when $\epsilon_3 = 3\epsilon_1$. This discrepancy might be explained by the same reasoning as in the previous example.

Finally, we consider the case of a diaphragm whose thickness D is a small but not infinitesimal fraction of a wavelength. In Fig. 5 the normalized junction susceptance is plotted as a function of D/λ_0 with the diaphragm height ratio d/b as a parameter and for $b_3 = 2b_1 = 2b$. The dielectric constant is unity in all three regions and the width of the first guide is $0.10\lambda_0$. It is remarkable that even for diaphragm thicknesses of $0.001\lambda_0$ the susceptance is noticeably larger than for the case when the thickness vanishes completely ($D/\lambda_0 = 0$). If $d/b = 0.50$ the former susceptance is 14 percent larger, but for $d/b = 0.25$ it is only 8 percent larger. Moreover, as the thickness increases beyond $0.01\lambda_0$ the susceptance rises quite rapidly. This could be attributed to the fact that the thicker diaphragm inhibits *reactive* energy in the higher order cutoff modes ($TM_1, TM_2, \cdots$) from tunneling through to the larger guide on the right where some of it could be converted into *real* energy of the TEM mode propagating away from the diaphragm. This energy is in large part retained in the neighborhood of the left side of the diaphragm, thereby contributing to the increase in junction susceptance as shown in Fig. 5. No

TABLE I
NORMALIZED LOAD ADMITTANCE FOR THE E-PLANE 2:1 STEP-DIAPHRAGM DISCONTINUITY OF FIG. 5 FOR $b = 0.10\lambda_0$ AND $\epsilon_1 = \epsilon_2 = \epsilon_3 = \epsilon_0$.

D/λ_0 \ d/b	0.25	0.50	0.75
0.000	0.500 + j0.201	0.500 + j0.327	0.500 + j0.592
0.001	0.501 + j0.219	0.501 + j0.376	0.501 + j0.748
0.010	0.510 + j0.291	0.509 + j0.501	0.507 + j1.000
0.030	0.542 + j0.443	0.540 + j0.752	0.535 + j1.518
0.100	0.857 + j1.047	0.871 + j1.812	0.860 + j3.787

attempt is made to plot the susceptance for diaphragm thicknesses greater than $0.1\lambda_0$ since the simple representation of a single shunt susceptance would clearly be unrealistic.

It is also of interest to consider the real part of the load admittance as "seen" by the smaller guide. The Ruehle and Lewin formula (see (11)) indicates that the very thin diaphragm affects only the junction susceptance and in a very simple way (compare (10) and (11)). This is confirmed by the present numerical results even for relatively large guide sizes and for thicker diaphragms. Only when the diaphragm thickness reaches $0.1\lambda_0$ does the real part of the admittance depart appreciably from 0.50 (normalized). Table I gives the load admittance information for the configuration of Fig. 5.

REFERENCES

[1] T Ruehle and L Lewin, "The E-plane st -diaphragm junction discontinuity," *IEEE Trans. Microwave Theory Te .1.*, vol. MTT-27, pp. 156–160, Feb. 1979
[2] J P Montgomery and L Lewin, "Note on an E-plane waveguide step with simultaneous change of media," *IEEE Trans. Microwave Theory Tech*, vol. MTT-20, pp. 763–764, Nov. 1972.
[3] L. Lewin, *Theory of Waveguides*. New York, Toronto: Halsted, 1975.
[4] R Safavi Naini and R H. MacPhie, "On solving w eguide junction scattering problems by the conservation of complex power technique,", *IEEE Trans. Microwave Theory Tech*, vol. MTT-29, pp 337–343, April 1981.
[5] R. Mittra and S W. Lee, *Analytic Techniques in the Theory of Guides Waves*. New York MacMillan, 1971
[6] N. Marcuvitz, Ed., *Waveguide Handbook*. New York: McGraw-Hill, 1951.

Multifrequency Cryogenically Cooled Front-End Receivers for the Westerbork Synthesis Radio Telescope

J. L. CASSE, E. E. M. WOESTENBURG, AND J. J VISSER

***Abstract*—Four of the fourteen 25-m antennas of the Westerbork Synthesis Radio Telescope have been equipped with 6- and 21-cm wavelength receivers based on cryogenically cooled parametric amplifiers and up-converters. Special care has been given to the design of the input network to achieve maximum sensitivity. An integrated feed launcher and preamplifier system are housed in a dewar at cryogenic temperatures. The**

Manuscript received July 16, 1981; revised Sept 14, 1981.
The authors are with the Netherlands Foundation for Radio Astronomy, Postbus 2, 7990 AA Dwingeloo, The Netherlands

0018-9480/82/0200-0201$00.75 ©1982 IEEE